Influence of End Group and Molecular Weight on Polybutadiene Fingerprint Secondary Ion Mass Spectra

X. Vanden Eynde* and P. Bertrand

Unité de Physico-Chimie et de Physique des Matériaux (PCPM), Université Catholique de Louvain, Place Croix du Sud 1, B-1348 Louvain-la-Neuve, Belgium

P. Dubois† and R. Jérôme

Center for Education and Research on Macromolecules (CERM), Université de Liège, Bât. B6, Sart-Tilman, B-4000 Liège, Belgium

Received May 4, 1998; Revised Manuscript Received June 26, 1998

ABSTRACT: Polybutadiene samples of different molecular weight have been synthesized by anionic polymerization as initiated by *sec*-butyllithium with low polydispersity and a major content of 1,2-vinyl units. They have been analyzed by time-of-flight secondary ion mass spectrometry (ToF-SIMS) in order to investigate the sensitivity of this method toward the *sec*-butyl end group and toward the molecular weight. The SIMS spectra show the characteristic fragment of the end group, $C_4H_9^+$ at $m/z = 57$, whose the peak intensity is strongly dependent on the polymer molecular weight, as is the case for almost all the fragment intensities. A model consistent with the peak intensity variations is used to give some new insights into the fragmentation mechanism at the end groups and within the main chain. Moreover, the analysis of the end group fragment allows M_n to be readily determined up to $M_n = 4 \times 10^4$ from, for example, the $Y_{(53)}/Y_{(57)}$ intensity ratio where $Y_{(53)}$ is the intensity of the deprotonated repeat unit ($[M - H]^+$). Other M_n calibration methods have also been used and are discussed in terms of their accuracy and physical meaning.

Introduction

Secondary ion mass spectrometry is now widely used to characterize the molecular structure and functionality of the surface of different polymer materials such as polymer blends, surface-treated polymers (plasma, chemical functionalization).[1] The chemical information is derived from the secondary molecular ions which are the fingerprints of the surface molecular structure. Many homopolymer spectra are now available in libraries of static secondary ion mass spectroscopy (SIMS) spectra.[2] The static SIMS has proven to be very useful in discriminating between many types of hydrocarbon polymers, such as polyethylene, polypropylene, polyisobutylene, and polystyrene,[3−5] in contrast to X-ray photoelectron spectroscopy (XPS), which requires a careful study of the valence band. This work is focused on the study of 1,2-polybutadiene (PB). Its SIMS fingerprint spectrum was previously studied for both secondary ion polarities and for both types of monomer units: 1,4-cis/trans and 1,2-vinyl.[3−6] The assignment of ion molecular structures to the main peaks is such that there is no peak characteristic of the 1,4- and 1,2-units, but rather, the relative peak intensity changes with the PB molecular structure.[6] As observed for other polymers, these relative intensities are expected to change with the molecular weight.

The molecular weight dependent fragmentation has been already studied for several polymers, such as polystyrene,[7−9] deuterated polystyrene,[10] poly(methyl methacrylate),[11] perfluoropolyether,[12−14] poly(ethylene glycol),[15] polycarbonate,[12,14] and many polyolefins.[16] In the polyolefin series, Galuska analyzed monodisperse 1,4-polybutadiene and proposed a nonlinear calibration curve for the M_n calculation from an intensity ratio accurate up to $M_n \approx 1 \times 10^4$.[16] Since the molecular structure of the end group was unknown, this author was unable to identify the end group characteristic fragments. Nevertheless, he proved that knowledge of M_n at the surface of polymeric materials was of great practical interest for applications. Indeed, low molecular weight polymers can be localized by imaging the surface. A first application concerns the composite materials, where short chain segregation has been observed to occur at the matrix−fiber interface, with detrimental effect on the adhesion.[17,16] Another example of this new capability of the time-of-flight (ToF) SIMS technique was the detection of defects in a polycarbonate CD-ROM surfaces due to a localized segregation of short polymer chains.[13]

Recently, we proposed a model able to account for the influence of the end groups on the absolute intensity of the characteristic polymer fragments and for the effect of molecular weight, as well. The molecular characteristic features actually influence the fragmentation. For instance, if a hydrogen end group is substituted by a *sec*-butyl one, the fragmentation is modified.[9] Minor modifications of the end group structure, such as isomerization, are also important, as proved by the analysis of polystyrene (PS)[8] and poly(butyl methacrylate)[18,19] containing different isomers of the butyl group. Indeed, for PS, aromatic species are formed when the secondary butyl isomer is the end group, in contrast to what happens when a tertiary butyl end group is used.[8] Lub et al. have also observed that the butyl isomer influences the formation of enolate fragments.[19] Indeed, the dehydrogenation cannot occur in the case of the *tert*-butyl enolates.

* Corresponding author. E-mail: vandeneynde@pcpm.ucl.ac.be.
† Current address: Services des Matériaux Polymères et Composites, Université de Mons-Hainaut, Place du Parc 20, B-7000 Mons, Belgium.

S0024-9297(98)00706-2 CCC: $15.00
Published on Web 09/03/1998

Scheme 1. Molecular Structure of the *sec*-PB-H

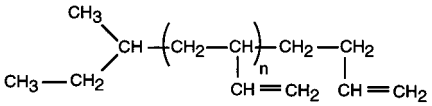

Table 1. Number-Average Molecular Weights (M_n), Polydispersity Coefficients ($H = M_w/M_n$), Determined by GPC, and 1,2-Vinyl %, Determined by ^{1}H NMR

	M_n	H	% 1,2-vinyl
sec-PB-H6K	6270	1.02	86
sec-PB-H11K	10800	1.01	86
sec-PB-H20K	19800	1.01	86
sec-PB-H40K	40180	1.01	86
tert-PB-H5K	5450	1.02	88

In SIMS, fragmentation of the polymer chains can occur according to different pathways depending on the mechanism of the energy deposition initiated by the impact of the primary ions.[20] The strong fragmentation of the polymer molecular structure leads to the emission of atomic or quasiatomic fragments. The chemical information derived from these ions is very poor. Another process is the direct scission of the polymer molecular structures and the emission of fragments in a charged state.[20] This gives straightforward molecular information based, for example, on the pendant group, end group, monomer, or dimer. A rearrangement of the molecular structure during the ion emission process can be caused by the internal energy deposited into the polymer chains. The ion beam interaction is a physical process, but the formation of a given fragment can be predicted by some general mass spectrometry and chemistry rules. Indeed, intense characteristic peaks are usually detected for very stable ion fragments. Many papers studied the SIMS fragmentation processes of polystyrene,[20−23] poly(ethylene terephthalate),[20,24,25] poly(vinyl methyl ether),[26] poly(tetrafluoroethylene),[27] and polyethylene.[28] Different experimental methods were used such as isotopic labeling, tandem mass spectrometry, and kinetic energy distribution. Analogy with the classical mass spectrometry was found.[29] Unfortunately, the classical mass spectrometry does not deal with negative ion fragments.[29] The analysis of molecular weight dependent fragmentation allows one to consider specific fragmentation processes initiated by the end group and then to interpret M_n effects as their specific fragmentation pathways. The purpose of this work is the ToF−SIMS analysis of several monodisperse polybutadiene samples of a predominantly 1,2-vinyl structure.

Materials and Methods

Polymer Synthesis. Monodisperse polybutadienes of a predominantly 1,2-vinyl structure and different molecular weights were synthesized by living anionic polymerization at the Center for Education and Research on Macromolecules (CERM, University of Liège). This polymerization was detailed in many textbooks.[30,31] *sec*-Butyllithium (or *tert*-butyllithium) was used as the initiator. The polymerization was stopped by the adjunction of methanol in order to attach a hydrogen as the ω-end group. The end group was a *sec*-butyl or a *tert*-butyl group, depending on the α-initiator (Scheme 1). The number-average molecular weight (M_n) and the polydispersity coefficients were measured by GPC for the different samples and they are listed in Table 1.

Sample Preparation. The polymer was first dissolved in tetrahydrofuran (THF; HPLC grade from UCB, Belgium), precipitated in methanol (HPLC grade from UCB, Belgium), and filtered. It was dissolved in THF (30 mg/mL) and thin films were prepared by spin coating a drop of this solution for 1 min (at 5000 rpm) onto a silicon wafer (used as received). No further treatment was applied before analysis. All films were free from cracks and defects and thick enough (≥∼5 nm) for the SSIMS spectra to be rid of the silicon signal (Si^+ at $m/z = 28$) of the substrate and of any substrate effects.[32] All samples were free from additives and small molecular weight compounds as supported by the lack of contribution in the spectra.

ToF-SIMS. The static SIMS measurements were carried out at UCL, Louvain-la-Neuve with a Charles Evans & Associates TFS-4000 MMI time-of flight spectrometer using a $^{69}Ga^+$ (15 keV) liquid metal ion source.[33] In this system, the secondary ions are accelerated at 3 keV before being deflected by 270° by three electrostatic hemispherical analyzers (TRIFT).[33] A 590 pA DC primary ion beam is pulsed at a 5 kHz frequency with a pulse width of 4 ns and is rastered over a 190 × 190 μm^2 surface area. All spectra were acquired during 10 min with a total fluence < 10^{12} ions/cm^2, ensuring static conditions. A mass resolution $m/\Delta m \sim 6000$ measured at $m/z = 28$ on a Si wafer was achieved. No charge neutralization was needed. For each sample, three or four spectra were acquired. To avoid experimental fluctuations, all the setting parameters were kept as constant as possible and all the spectra were acquired the same day. Moreover, our analysis was focused on the positive secondary ions which contain the most interesting information.

Data Treatment and Normalization. All the spectra were treated with the Cadence 2.0 software from Charles Evans & Associates. For each of the peaks contributing to a given spectrum (j), the absolute intensity $Y_{(i,j)}$ was measured and a unique ion composition (i) was assigned. As much as possible, the metastable peaks were not involved into the data set.[23] No major peak due to the polymer oxidation was observed in the positive and negative SIMS spectra.

The reproducibility of the absolute and normalized intensities was tested by measuring the standard deviation for each variable (intensity $Y_{i,j}$) with at least four independent measurements. A standard deviation of 8−15% of the mean absolute intensity was found. To define the number of repeat units, the GPC data were reprocessed. The number of repeat units in the polymer was calculated from M_n, where the end group masses were subtracted and the result was divided by the monomer molecular weight (54 g/mol).

As was shown in a previous paper, the total intensity cannot be used as a normalization parameter because it varies with M_n.[8] Then, the absolute intensities were considered rather than the normalized ones. This was made possible by the good reproducibility of the absolute intensities obtained within a short period of time.

To compare the quantitative efficiency of the calibration, we used the root mean square error of calibration (RMSEC).[34] This parameter is defined as:

$$\mathrm{RMSEC} = \sqrt{\sum_{i=1}^{n} \frac{(y_i - \hat{y}_i)^2}{n}} \qquad (1)$$

where y_i and $\hat{y}_i$ represent the experimental and the predicted $\langle n \rangle$ values, respectively.

Results

The positive SIMS spectra of a low and a high molecular weight polybutadiene are displayed in Figure 1. The characteristic fragments are similar to those already observed in the literature, namely, CH_2^+, $C_2H_3^+$, $C_3H_3^+$, $C_3H_5^+$, $C_4H_5^+$ or $[M - H]^+$, $C_4H_7^+$ or $[M + H]^+$, $C_5H_7^+$, $C_6H_5^+$, $C_6H_7^+$, $C_7H_7^+$, $C_8H_9^+$, and $C_9H_9^+$ at m/z = 14, 27, 39, 41, 53, 55, 67, 77, 79, 91, 105, and 117, respectively.[2,6] The characteristic fragment of the butyl end group was already determined for the polystyrene system.[8] The parent fragment is observed at $m/z = 57$

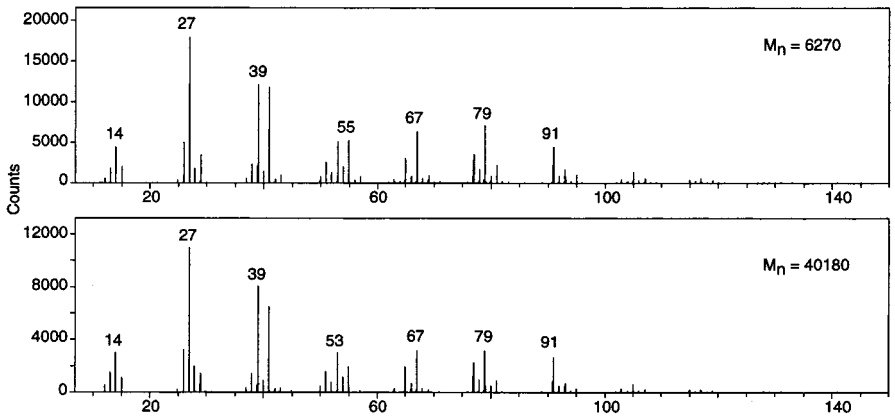

Figure 1. Positive SIMS spectra of low and high molecular weight *sec*-PB-H (m/z = 7−150): (a) *sec*-PB-H6K and (b) *sec*-PB-H40K.

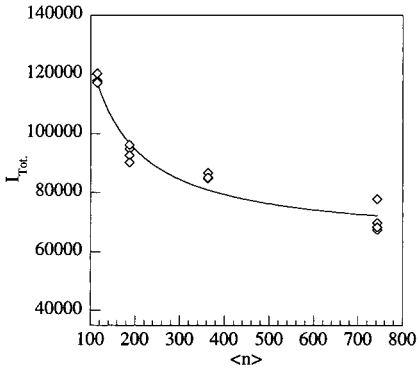

Figure 2. Positive total intensity versus the number of repeat units ($\langle n \rangle$).

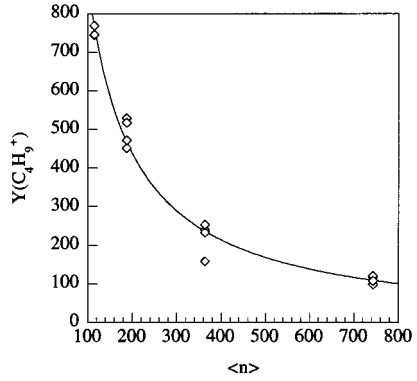

Figure 3. *sec*-butyl parent end group ion intensity ($Y_{(57)}$) vs the number of repeat units ($\langle n \rangle$).

with the $C_4H_9^+$ molecular structure. In the low M_n SIMS spectrum, the peaks at m/z = 57, 55, 69 exhibit higher intensities compared to the high molecular weight PB. In fact, almost all the peak intensities increase when the molecular weight is decreased.

Figure 2 shows the total intensity as a function of the mean number of repeat units ($\langle n \rangle$). When the molecular weight increases, $I_{Tot.}$ is observed to decrease. A similar trend is seen in Figure 3 for the parent end group ion at m/z = 57. This decrease seems to approach zero for an infinite molecular weight.

The absolute intensities of the fragments $C_2H_5^+$, $C_4H_5^+$ or $[M - H]^+$, $C_4H_7^+$ or $[M + H]^+$, and $C_5H_7^+$ at m/z = 29, 53, 55, and 67, respectively, are shown in Figure 4. It is worth noting that not only the parent butyl end group peak depends on the PB molecular weight but the intensity of most characteristic fragments vary. But at high molecular weights, these intensities remain significant.

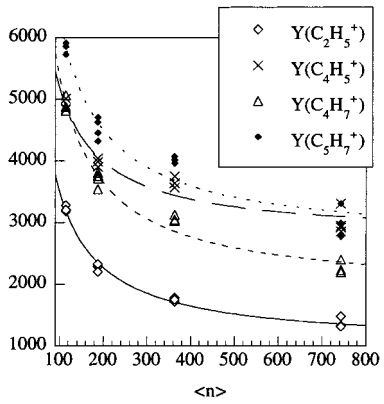

Figure 4. Peak intensities of the characteristic PB fragments vs the number of repeat units ($\langle n \rangle$).

The spectra for a *tert*-butyl PB (Figure 5) is similar to the *sec*-butyl PB ones shown in Figure 1. The characteristic polybutadiene peaks are the same except for the m/z = 57 peak, which seems much more intense for the *tert*-butyl PB than for the *sec*-butyl one. Indeed, the intensity of $C_4H_9^+$ at m/z = 57 is larger than expected for the *sec*-butyl PB, with an average molecular weight of ca. 5500 (Figure 5). Quantitatively, the change of the *sec*-butyl by a *tert*-butyl isomer results in a 6.5-fold increase of the absolute $C_4H_9^+$ peak intensity.

Discussion

In a previous paper, a model was proposed to describe the molecular weight dependence of the peak intensities in static SIMS spectra.[8] The aim of this model was to account for two phenomena observed during these experiments: the effect of M_n on the end group ion intensity and the end group interaction with the adjacent repeat unit. In this model, the absolute intensity of any ion fragment (X) is given by eq 2,

$$Y_X = \frac{A}{n+2} + \frac{Bn}{n+2} \qquad (2)$$

where A and B are parameters for the end group and the main chain, respectively. These parameters are independent of the number of repeat units ($\langle n \rangle$). It was shown that the A parameter accounts for the contribution of the fragments associated with the end groups through direct scission or rearrangement processes.[8] On the contrary, the B parameter is characteristic of

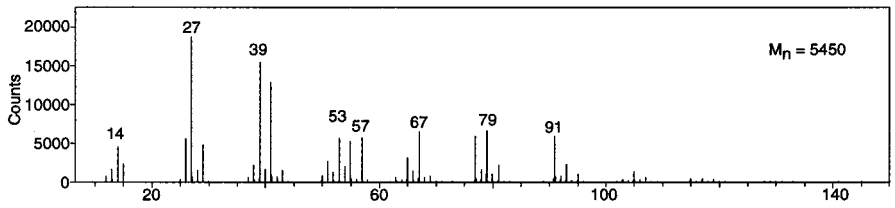

Figure 5. Positive SIMS spectrum of low and high molecular weight *tert*-PB-H5K ($m/z = 7-150$).

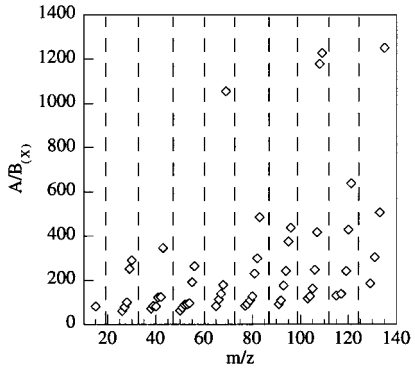

Figure 6. Influence of the *sec*-butyl end groups on the absolute intensities, $A/B_{(X)}$ ratios. The *sec*-butyl end group peak is not shown because its $A/B_{(X)}$ value is infinity.

fragmentation of the polymer main chain.

The full lines shown in Figures 2−4 result from the fitting of the data by this model. Since the $C_4H_9^+$ peak intensity decreases and approaches zero when the number of repeat units is increased, its *B* parameter is equal to zero, in the case of polybutadiene. Thus, in contrast to what was observed for polystyrene, there is no intensity contribution of the hydrocarbon contamination to the parent end group peak.[8,10] All the other fragments exhibit a nonzero value for the *B* parameter, showing that they are partially formed within the main chain. So all the polybutadiene fragments are influenced by changing the polymer molecular weight and, then, by the presence of the *sec*-butyl or hydrogen end groups, as well.

The influence of the end groups on the absolute intensity of an X fragment can be studied by another interesting output of our model, the $A/B_{(X)}$ ratio.[8] This ratio allows the end group interaction to be quantitatively characterized. A high $A/B_{(X)}$ ratio means a great influence of the end group on the secondary X ion emission. On the contrary, a low *A*/*B* value indicates that the end group has no or only a small effect on the ion yield. Figure 6 shows the value of the $A/B_{(X)}$ ratio for all the fragments detected in the spectra as a function of their mass-to-charge ratio (m/z). Clearly, the $A/B_{(X)}$ ratio of the fragments, present in each $C_nH_y^+$ cluster, increases with the hydrogen content. It can be assumed that the formation of saturated fragments depends on the presence of the *sec*-butyl and hydrogen end groups.

Different fragmentation pathways have to be considered for the formation of the end group, main chain, and rearranged fragments. First, some secondary molecular ions can be produced by direct scission of the molecular structure either at the hydrogen end group side, such as $C_3H_5^+$ and $C_4H_7^+$ or $[M + H]^+$, at $m/z = 41$ and 55, respectively, or at the butyl end group side, such as $C_4H_9^+$, $C_2H_5^+$, and CH_3^+ at $m/z = 57$, 29, and 15, respectively (see Scheme 2). Other fragments can also be produced by a direct scission in the main chain such

Scheme 2. End Group Scissions

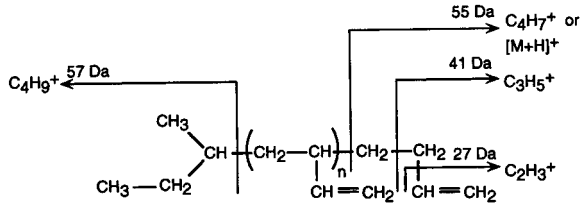

as, for example, $C_2H_3^+$, $C_4H_5^+$ or $[M - H]^+$, and $C_5H_9^+$ at $m/z = 27$, 53, and 69, respectively. Another possible pathway consists of the rearrangement of the precursor before/during the secondary ion emission. Such fragments can be produced by the rearrangement of the end group with the first adjacent repeat unit or by rearrangement of two repeat units. As an example, some protonated repeat unit fragments, $[M + H]^+$, could be formed by two adjacent repeat units. This pathway can be described by the rules valid for the classical mass spectrometry, as explained below.

In the case of the *sec*-butyl end group, a similar influence of molecular weight on all the peaks has been observed for both SIMS spectra of PS and PB.[8] The hydrogen transfer is thought to be one of the pathways promoted by the activation of the species around the primary ion impact area. This H transfer can be induced by the McLafferty's rearrangement occurring between the butyl end group and the first adjacent repeat unit. In this frame, the H transfer occurs through a six-membered ring transition and is at the origin of a fragmentation pathway, leading to the formation of more saturated species. After the H atom is transferred and before the scission at the butyl end group occurs, two different conformations have to be considered.[29] The first one is called charge or radical retention and the second one is charge or radical migration. The stability of the transition states decides which pathway is most favorable. As shown in Scheme 3, the radical is not stabilized by the electron-donating effect of the adjacent functionality so that the radical migration is not favored. Therefore, the promoted transition state is the radical retention. Then the protonated repeat unit fragments can be formed by the direct scission of the H end group and by the rearrangement mechanism of the *sec*-butyl end group with the first adjacent repeat unit.

The fragmentation within the main chain can also be discussed in terms of an hydrogen transfer between two adjacent repeat units through a similar six-membered ring transition state (Scheme 4). This mechanism leads to the formation of protonated and deprotonated repeat unit fragments. Since the radical migration provides a radical with a better stability, the deprotonated repeat fragment is favored. Moreover, the loss of one hydrogen atom might also be a more probable event than the gain of one H during the sputtering/emission process. Indeed, the H recombination with a sputtered fragment requires correlations in time, velocity, and space. Fi-

Scheme 3. End Group Rearrangements

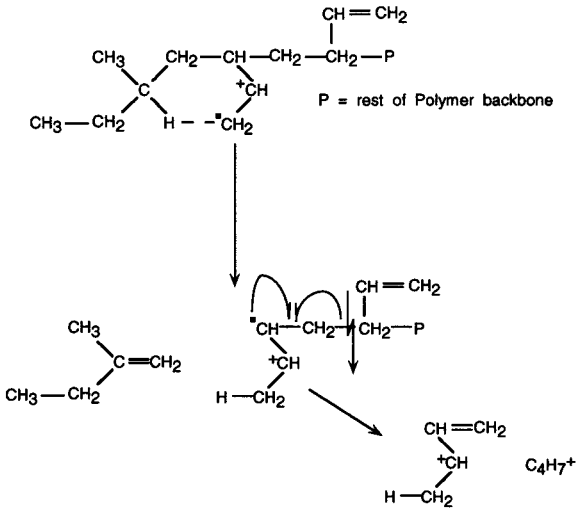

Scheme 4. Main Chain Rearrangements

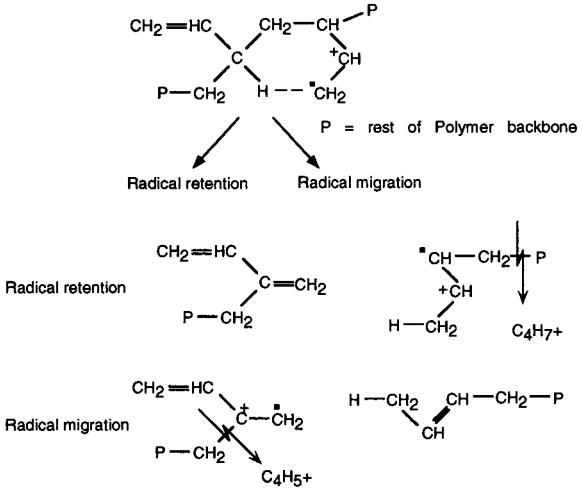

nally, the intensity of the main chain fragments could be influenced by other parameters, such as the kinetics of the ion formation.[13] In the range of the investigated PB molecular weights, this effect is not prominent, consistent with the linear and not the quadratic dependence of the characteristic intensity ratio on the number of repeat units, as will be shown later on.

In the literature, several parameters were used to characterize polybutadiene surfaces. They were proposed by van Ooij and modified by Briggs.[3,4] One of these parameters is $\sum C_8/\sum C_2$, where $\sum C_8$ and $\sum C_2$ are the sums of all the peak intensities in the clusters of fragments containing eight and two carbon atoms, respectively. Figure 7 illustrates the dependence of the $\sum C_8/\sum C_2$ ratio on the number of monomer units, i.e., a decrease when the number of monomer units is increased. This ratio is the complex result of several contributions, as can be seen in Figure 6 for the $A/B_{(X)}$ ratio. Indeed, all the peaks that contribute to the sums originate from different fragmentation pathways and are thus representative of many different precursors at the surface. A conclusion about this ratio is that the low molecular weight polymers favor the high mass fragments.

Another parameter used is the sum of the aromatic peaks. When the absolute peak intensities of the aromatic fragments ($C_6H_5^+$, $C_7H_7^+$, $C_8H_7^+$, $C_8H_9^+$, $C_9H_7^+$, $C_{10}H_8^+$ at m/z = 77, 91, 103, 105, 115, 128) are summed

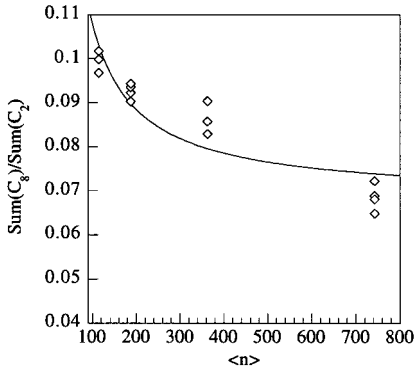

Figure 7. $\sum C_8/\sum C_2$, with $\sum C_8$ and $\sum C_2$ being the sums of all the peak intensities in the clusters of fragments containing eight and two carbon atoms, respectively, as a function of the number of repeat units.

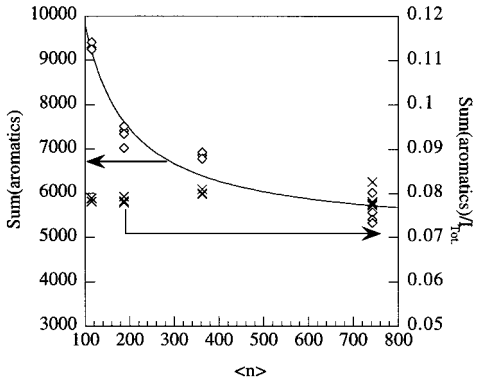

Figure 8. Sum of aromatic peaks vs the number of repeat units ($\langle n \rangle$): (a) absolute intensities and (b) normalized by the total intensity.

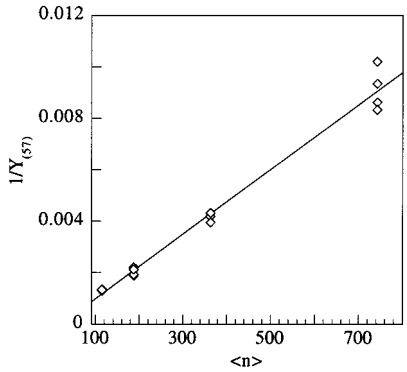

Figure 9. Inverse of $Y_{(57)}$ vs the number of repeat units ($\langle n \rangle$).

up, this sum increases for the low molecular weight polymers, but when it is normalized by the total intensity, the ratio remains constant (Figure 8). As for the $\sum C_8/\sum C_2$ parameter, the aromatic sum is difficult to interpret. Indeed, when the absolute intensities are considered, the aromatic fragments seem to be promoted by the end groups. However, when the peak intensities are normalized by $I_{Tot.}$, it is no longer the case for low molecular weight polybutadiene. In summary, these two empirical parameters cannot provide straightforward information and have to be basically considered as diagnostic tools.

Now, different methods will be discussed for the calibration of molecular weight based on the knowledge of the end group characteristic fragment, $C_4H_9^+$ at m/z = 57. In Figure 9, the inverse of $Y_{(57)}$ is plotted as a function of the average number of repeat unit. The $1/Y$

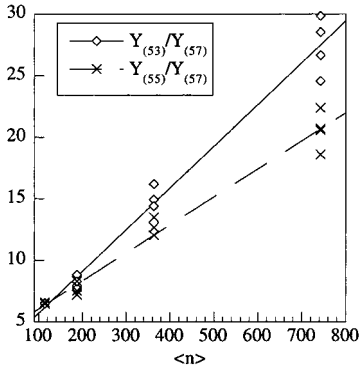

Figure 10. Intensity ratios $Y_{(55)}/Y_{(57)}$ and $Y_{(53)}/Y_{(57)}$ vs the number of repeat units ($\langle n \rangle$).

data show a linear dependence on $\langle n \rangle$. Since there is no interference with the repeat units, the absolute end group intensity can be directly used for the M_n determination, thus independently of any data pretreatment.[8] The model fits the linear relationship between an end group fragment and the number of repeat units in the main chain (eq 3).

$$\frac{1}{Y_{EG}} = \frac{n+2}{A'} \tag{3}$$

Nevertheless, this method is not very useful because it needs very good reproducibility of the absolute intensity measurements over long periods of time. This condition is usually not fulfilled because of sample roughness, surface charging, and fluctuations of the mass spectrometer. All these artifacts can induce large variations in the absolute intensities, which can, however, be avoided if the spectra are normalized by an appropriate parameter, such as a main chain fragment.[35]

The intensity ratios $Y_{(53)}/Y_{(57)}$ and $Y_{(55)}/Y_{(57)}$ are displayed in Figure 10, where $Y_{(53)}$ and $Y_{(55)}$ (equivalent to Y_{MC}) are the main chain peak intensities and $Y_{(57)}$ (equivalent to Y_{EG}) is the intensity of the end group characteristic peak. These ratios show a linear dependence on $\langle n \rangle$ and with a positive offset at $\langle n \rangle = 0$. The main parameter for the molecular weight determination is the characteristic end group intensity. The main chain does not seem to be important and, indeed, the linear dependence is observed for any main chain peak. If the main chain fragment is influenced by the end group, the intensity ratio between the main chain and the end group would still agree with a linear dependence on $\langle n \rangle$ and a positive offset (A/A') could be observed (eq 4). It should be noticed that this relationship cannot deal with $\langle n \rangle = 0$, since the A parameter takes into account the fragment formed by the end group or its interaction with the first adjacent repeat unit. Then, obviously, our model is consistent with $\langle n \rangle$ being higher than two.

$$\frac{Y_{MC}}{Y_{EG}} = \frac{A}{A'} + \frac{Bn}{A'} \tag{4}$$

In Figure 11, the *X*-axis is the *B* parameter values calculated by fitting the absolute intensities with eq 2 and the *Y*-axis is the slope coefficient derived from the linear fit of the $Y_{(X)}/Y_{EG}$ intensity ratio for all the PB fragments. It can be seen that these two quantities are directly proportional to a coefficient of 1.25 10^{-5} which

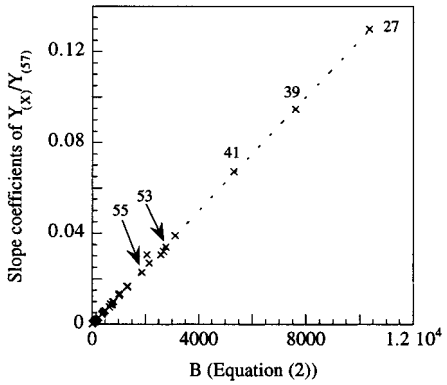

Figure 11. *B* parameters (obtained from fitting $Y_{(X)}$ with eq 2) vs the slope coefficients of $Y_{(X)}/Y_{(57)}$ (linear fit).

Table 2. Correlation Coefficents and Root Mean Square Error of Calibration (RMSEC) for the Different M_n Determination Methods

	linear slope coefficients	correlation coefficient	RMSEC
$1/Y_{(57)}$	1.251×10^{-5}	0.992	8.2
$Y_{(53)}/Y_{(57)}$	0.0339	0.990	8.9
$Y_{(55)}/Y_{(57)}$	0.0228	0.988	10
$(Y_{(53)} + Y_{(55)})/Y_{(57)}$	0.0567	0.989	8.2
$Y_{(27)}/Y_{(57)}$	0.130	0.992	6.99
$Y_{(55)}/Y_{(27)}$ nonlinear (eq 6)		0.994	10.3

gives an estimation of the $(A')^{-1}$ parameter (see eq 4). The $(A')^{-1}$ parameter can also be derived from the eq 3 and is estimated to 1.22 10^{-5} in Figure 9. The good agreement between these two values supports the consistency of the model with the data.

To check the accuracy of the fits and ratios, two parameters were used: the correlation coefficient and the root-mean-square error of calibration (RMSEC) which evaluate the validity of the fit and the error interval of the fit. The RMSEC is restricted to the range of the calibration data. All the RMSEC and correlation coefficients are listed in Table 2. The RMSEC($Y_{(53)}/Y_{(57)}$) value is smaller than the RMSEC($Y_{(55)}/Y_{(57)}$) value. The RMSEC($Y_{(27)}/Y_{(57)}$) value is found to be smaller than for the repeat unit fragments. The RMSEC decreases as the slope of the linear fit increases. From eq 4, the slope depends on the intensity of the main chain fragment or the *B* parameter (eq 2). Therefore, the most intense main chain fragment, $C_2H_3^+$ (at $m/z = 27$), leads to the best M_n calibration (lower RMSEC) compared to the other fragments, whatever the influence of the end groups on their intensity.

To compare our results with those published by Galuska, the $Y_{(55)}/Y_{(27)}$ intensity ratio measured by this author is shown as a function of the molecular weight logarithm (Figure 12, where $Y_{(55)}$ and $Y_{(27)}$ represents the absolute intensities of the fragments $C_4H_7^+$ and $C_2H_3^+$ at $m/z = 55$ and 27, respectively).[16] The ratio decreases when the average number of repeat units is increased. Two different fits are also displayed in this figure and the error parameters are listed in Table 2. Galuska proposed a model based on the relationship between the molecular weight and the polymer radius of gyration in order to explain the M_n effect on the SIMS spectra. The equation proposed by Galuska can be written as follows.[16]

$$\frac{Y_{(55)}}{Y_{(27)}} = M\left(\frac{M_W}{1000}\right)^E + B \tag{5}$$

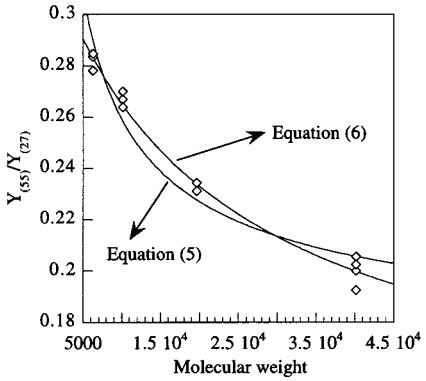

Figure 12. Intensity ratio $Y_{(55)}/Y_{(27)}$ vs the logarithm of the molecular weight. The continuous and dashed lines are for the eq 6 and Galuska's fits eq 5, respectively.

where M_W represents the weight-average of molecular weight, M and B are constants of the fits and the exponent, E, is fixed at -0.6 by the model.[16]

The second fit shown in Figure 12 is a nonlinear fit based on the eq 6, which is based on the ratio between two peak intensities ($Y_{(X1)}$ and $Y_{(X2)}$) that both follow the eq 2.

$$\frac{Y_{X_1}}{Y_{X_2}} = \frac{A + Bn}{A'' + B''n} \tag{6}$$

The correlation coefficient and the RMSEC observed for this fit are 0.994 and 10.3, respectively. This nonlinear fit takes more parameters into account and gives better results, supporting that the best calibration curve is obtained with the nonlinear fit of eq 6. Galuska's model is a geometrical model for the end group concentration at the surface, which does not take into account the matrix effect for the end group ion formation. The differences in the two independent studies of PB could result from some differences in the PB microstructure. Moreover, the molecular weight range, covered by this precedent study, is broader than in this study.

Although fragmentation of PB in relation to molecular weight dependence and end group has been clear up, some questions are still pending, such as the effects of the 1,4-cis/trans microstructure on the rearrangements and the influence of chain stereoregularity on the polybutadiene surfaces as previously studied for PS and PMMA.[36] Moreover, the higher intensity for the *tert*-butyl fragment is explained by the higher stability of the carbocation due the inductive effect of the three methyl groups (electron donators). This means that the secondary ion yield for $C_4H_9^+$ at $m/z = 57$ depends on the isomer precursor. By using the Y_{MC}/Y_{EG} intensity ratio, the upper limit for the accurate molecular weight determination is expected to be increased by the use of a more sensitive end group, such as a *tert*-butyl one.[8,37]

Conclusion

The influence of molecular weight on the static SIMS spectra of polybutadiene has been shown. This dependence has been explained by the effect of the molecular structure of the polymer and the butyl end groups and by the interaction of the end group with the first adjacent repeat units. The observations reported for the 1,2-vinyl polybutadiene confirm previous conclusions drawn for PS and validate a model proposed in this study. It is now clear that the end group molecular structure and the polymer molecular weight play an important role in the formation of the secondary ion.

A simple model was used to quantify the contributions of both the main chain and the end group to the peak intensities. According to this model, it was found that, in each cluster, the more hydrogenated fragments are more dependent on the molecular weight, pointing out the role of the H transfer in their formation. Moreover, some fragmentation mechanism have been proposed that are in agreement with the usual mass spectrometry schemes.

The polybutadiene molecular weight has been successfully calibrated on a linear scale, since the molecular structure of the end groups was known and the molecular structure of the polybutadiene samples was kept unchanged. The characteristic fragment of the *sec*-butyl end group is detected at $m/z = 57$ and the molecular structure assigned is $C_4H_9^+$. The inverse of the *sec*-butyl peak intensities allows the direct calibration of M_n using a linear relationship with the average number of repeat units per chain up to $M_n \approx 40000$. Several other intensity ratios give similar results.

Acknowledgment. The financial support from the "Fonds National de la Recherche Scientifique (FNRS)-Loterie Nationale" (Belgium) and from the "Région Wallonne" (Belgium) for the acquisition of the ToF-SIMS spectrometer is gratefully acknowledged. This work is sponsored in part by the Belgian Interuniversity Attraction Pole Program on "Reduced Dimensionality Systems" (PAI-IUAP P4/10) and on "Supramolecular Chemistry and Catalysis" (PAI-IUAP P4/11).

References and Notes

(1) Benninghoven, A. *Angew. Chem., Int. Ed. Engl.* **1994**, *33*, 1023. Gardella, J. A.; Pireaux, J. J. *Anal. Chem.* **1990**, *62*, 645A. Vickerman, J. C. *Analyst* **1994**, *119*, 513. van Leyen, D.; Hagenhoff, B.; Niehuis, E.; Benninghoven, A.; Bletsos, I. V.; Hercules, D. M. *J. Vac. Sci. Technol. A* **1989**, *7/3*, 1790. Briggs, D. *Surf. Interface Anal.* **1982**, *4*, 151. Short, R. D.; Ameen, A. P.; Jackson, S. T.; Pawson, D. J.; O'Toole, L.; Ward, A. J. *Vacuum* **1993**, *44*, 1143. Vickerman, J. C.; Leggett, G. J.; Hagenhoff, B.; Briggs, D.; Chilkoti, A.; Bryan, S. R.; McKeown, P. J. In *Wiley Static SIMS Library*; Surface Spectra: Manchester, 1997. Vickerman, J. C.; Swift, A. In *Surface Analysis: the principal techniques*; Vickerman, J. C., Ed., John Wiley & Sons: 1997; p 135. Wien, K. *Nucl. Instrum. Methods* 1997, B131, 38. Bertrand, P.; Weng, L. T. In *Surface Characterization: A Practical Approach*; Scandinavian Scientific Press and VCH Publishers: 1997. Weng, L. T.; Bertrand, P. *Mikrochem. Acta* **1996**, *Suppl. 13*, 167.

(2) Newman, J. G.; Carlson, B. A.; Michael, R. S.; Moulder, J. F.; Holt, T. H. In *Static SIMS Handbook of Polymer Analysis*; Perkin-Elmer Corp.: Eden Prarie, 1991. Briggs, D.; Brown, A.; Vickerman, J. C. In *Handbook of Static Secondary Ion Mass Spectrometry (SIMS)*; John Wiley & Sons: New York 1989.

(3) van Ooij, W. J.; Brinkhuis, R. H. G. *Surf. Interface Anal.* **1988**, *11*, 430.

(4) Briggs, D. *Surf. Interface Anal.* **1990**, *15*, 734.

(5) Delcorte, A.; Weng, L. T.; Bertrand, P. *Nucl. Instrum. Methods B* **1995**, *46*, 213.

(6) Weng, L. T.; Bertrand, P.; Lauer, W.; Zimmer, R.; Busetti, S. *Surf. Interface Anal.* **1995**, *23*, 879.

(7) Vanden Eynde, X.; Weng, L. T.; Bertrand, P. In *Proceedings of the 10th International Conference on Secondary Ion Mass Spectrometry SIMS X*; Benninghoven, A., Hagenhoff, B., Werner, H. W., Eds.; J. Wiley & Sons: New York, 1997; p 727.

(8) Vanden Eynde, X.; Bertrand, P.; Jérôme, R. *Macromolecules* **1997**, *30*, 6407.

(9) Vanden Eynde, X.; Matyjaszewski, K.; Bertrand, P. *Surface Interface Anal.* **1998**, *26*, 569.

(10) Vanden Eynde, X.; Reihs, K.; Bertrand, P. In *Proceedings of the 11th International Conference on Secondary Ion Mass Spectrometry, SIMS XI*; Gillen, G., Lareau, R., Bennett, J., Stevie, F., Eds.; J. Wiley & Sons: New York, 1997; p 571.
(11) Leeson, A. M.; Alexander, M. R.; Short, R. D.; Briggs, D.; Hearn, M. J. *Surf. Interface Anal.* **1997**, *25*, 261.
(12) Reihs, K.; Voetz, M.; Kircher, K.; Deimel, M.; Petrat, F. M.; Wolany, D.; Benninghoven, A. In *Proceedings of the 10th International Conference on Secondary Ion Mass Spectrometry*; Benninghoven, A., Hagenhoff, B., Werner, H. W., Eds.; J. Wiley & Sons: New York, 1997; p 641.
(13) Reihs, K.; Voetz M.; Kruft M.; Wolany D.; Benninghoven, A. *Fresenius J. Anal. Chem.* **1997**, *358*, 93.
(14) Fowler, D. E.; Johnson, D.; Vanleyen, D.; Benninghoven, A. *Surf. Interface Anal.* **1991**, *17*, 125.
(15) Shard, A. G.; Davies, M. C.; Schacht, E. *Surf. Interface Anal.* **1996**, *24*, 787.
(16) Galuska, A. A. *Surf. Interface Anal.* **1997**, *25*, 790.
(17) Poleunis, C.; Fallais, I.; Carlier, V.; Sclavons, M.; Bertrand, P.; Legras, R. In *Proceedings of the 10th International Conference on Secondary Ion Mass Spectrometry*; Benninghoven, A., Hagenhoff, B., Werner, H. W., Eds.; J. Wiley & Sons: New York, 1997; p 173.
(18) Castner, D. G.; Ratner, B. D. *Surf. Interface Anal.* **1990**, *16*, 479.
(19) Lub, J.; van der Wel, H. *Org. Mass Spectrom.* **1990**, *25*, 588.
(20) Leggett, G. J.; Vickerman, J. C. *Int. J. Mass Spectrosc. Ion. Proc.* **1992**, *122*, 281.
(21) Affrossman, S.; Hartshorne, M.; Jérôme R.; Munro, H.; Pethrick, R. A.; Petitjean, S.; Vilar, M. R. *Macromolecules* **1993**, *26*, 5400.
(22) Chilkoti, A.; Castner, D. G.; Ratner, B. D. *Appl. Spectroscopy* **1991**, *45/2*, 209.
(23) Delcorte, A.; Segda, B. G.; Bertrand, P. *Surf. Sci.* **1997**, *381*, 18.
(24) Leggett, G. J.; Vickerman, J. C.; Briggs, D.; Hearn, M. J. *J. Chem. Faraday Trans.* **1992**, *88* (3), 297.
(25) Ramsden, W. D. *Surf. Interface Anal.* **1991**, *17*, 793.
(26) Leggett, G. J.; Chilkoti, A.; Ratner, B. D.; Vickerman, J. C. *Surf. Interface Anal.* **1992**, *18*, 210.
(27) Leggett, G. J.; Briggs, D.; Vickerman, J. C. *J. Chem. Faraday Trans.* **1990**, *86* (10), 1863.
(28) Leggett, G. J.; Briggs, D.; Vickerman, J. C. *Surf. Interface Anal.* **1991**, *17*, 737.
(29) McLafferty, F. W.; Turecek, F. In *Interpretation of Mass Spectra*, 4th ed.; University Science Books: 1993.
(30) Painter, P. C.; Coleman, M. M. In *Fundamentals of Polymer Sciences*; Technomic Publishing: Sausalito, 1994.
(31) Young, R. N.; Quirk, R. P.; Fetters, L. J. *Adv. Polym. Sci.* **1984**, *56*, 1.
(32) Delcorte, A.; Bertrand, P.; Arys, X.; Jonas, A.; Wischeroff, E.; Mayer, B.; Laschewsky, A. *Surf Sci.* **1996**, *366*, 149.
(33) Schueler, B. W. *Microsc. Microanal. Microstruct.* **1992**, *3*, 119.
(34) Vanden Eynde, X.; Bertrand, P. *Surf. Interface Anal.* **1997**, *25*, 878.
(35) Vanden Eynde, X.; Bertrand, P. *Surf. Interface Anal.* **1998**, *26*, 579.
(36) Vanden Eynde, X.; Weng, L. T.; Bertrand, P. *Surf. Interface Anal.* **1997**, *25*, 41.
(37) Vanden Eynde, X.; Fallais, I.; Devaux, J.; Bertrand, P. In *Proc. International Conference on Polymer-Solid Interface*, 2nd ed.; Pireaux, J.-J., Delhalle, J., Rudolf, P., Eds; Presses Universitaires de Namur: Namur, 1998; p 473.

MA9807062